TOPICAL REVIEW

Developments in magnetocaloric refrigeration

INSTITUTE OF PHYSICS PUBLISHING JOURNAL OF PHYSICS D: APPLIED PHYSICS

J. Phys. D: Appl. Phys. **38** (2005) R381–R391 doi:10.1088/0022-3727/38/23/R01

TOPICAL REVIEW

Developments in magnetocaloric refrigeration

Ekkes Brück

Van der Waals-Zeeman Instituut, Universiteit van Amsterdam, Valckenierstraat 65, 1018 XE Amsterdam, The Netherlands

Received 5 October 2005
Published 18 November 2005
Online at stacks.iop.org/JPhysD/38/R381

Abstract

Modern society relies on readily available refrigeration. Magnetic refrigeration has three prominent advantages compared with compressor-based refrigeration. First, there are no harmful gases involved; second, it may be built more compactly as the working material is a solid; and third, magnetic refrigerators generate much less noise. Recently a new class of magnetic refrigerant-materials for room-temperature applications was discovered. These new materials have important advantages over existing magnetic coolants: they exhibit a large magnetocaloric effect (MCE) in conjunction with a magnetic phase-transition of first order. This MCE is larger than that of Gd metal, which is used in the demonstration refrigerators built to explore the potential of this evolving technology. In the present review we compare the different materials considering both scientific aspects and industrial applicability. Because fundamental aspects of MCE are not so widely discussed, we also give some theoretical considerations.

(Some figures in this article are in colour only in the electronic version)

1. Introduction

Magnetic refrigeration, based on the magnetocaloric effect (MCE), has recently received increased attention as an alternative to the well-established compression–evaporation cycle for room-temperature applications. Magnetic materials contain two energy reservoirs; the usual phonon excitations connected to lattice degrees of freedom and magnetic excitations connected to spin degrees of freedom. These two reservoirs are generally well coupled by the spin lattice coupling that ensures loss-free energy transfer within millisecond time scales. An externally applied magnetic field can strongly affect the spin degree of freedom that results in the MCE. In the magnetic refrigeration cycle, depicted in figure 1, initially randomly oriented magnetic moments are aligned by a magnetic field, resulting in heating of the magnetic material. This heat is removed from the material to the ambient by heat transfer. On removing the field, the magnetic moments randomize, which leads to cooling of the material below ambient temperature. Heat from the system to be cooled can then be extracted using a heat-transfer medium. Depending on the operating temperature, the heat-transfer medium may be water (with antifreeze) or air, and for very low temperatures, helium. Therefore, magnetic refrigeration is an environmentally friendly cooling technology. It does not use ozone depleting chemicals (CFCs), hazardous chemicals (NH_3) or greenhouse gases (HCFCs and HFCs). Another key difference between vapour-cycle refrigerators and magnetic refrigerators is the amount of energy loss incurred during the refrigeration cycle. The cooling efficiency in magnetic refrigerators working with gadolinium has been shown [1] to reach 60% of the theoretical limit, compared with only about 40% in the best gas-compression refrigerators. This higher energy efficiency will also result in a reduced CO_2 release. Current research aims at new magnetic materials displaying larger MCEs, which then can be operated in fields of about 2 T or less, that can be generated by permanent magnets.

The heating and cooling described above is proportional to the change of magnetization and the applied magnetic field. This is the reason why, until recently, research in magnetic refrigeration was almost exclusively conducted on superparamagnetic materials and on rare-earth compounds [2].

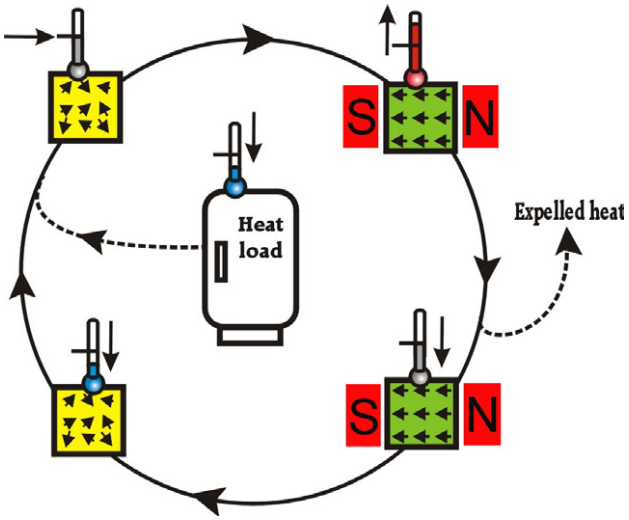

Figure 1. Schematic representation of a magnetic-refrigeration cycle, that transports heat from the heat load to the ambient. Left and right depict material in low and high magnetic field, respectively.

For room-temperature applications like refrigerators and air-conditioners, compounds containing manganese should be a good alternative. Manganese is a transition metal with high abundance. Also, there exist in contrast to rare-earth compounds, an almost unlimited number of manganese compounds with critical temperatures near room temperature. However, the magnetic moment of manganese generally is only about half the size of heavy rare-earth elements. Enhancement of the caloric effects associated with magnetic moment alignment may be achieved through the induction of a first order phase-transition or better a very rapid change of magnetization at the critical temperature, which will bring about a much higher efficiency of the magnetic refrigerator. In combination with currently available permanent magnets, this opens the path to the development of small-scale magnetic refrigerators, which no more rely on rather costly and service-intensive superconducting magnets. Another prominent advantage of magnetocaloric refrigerators is that the cooling power can be varied by scaling from milliwatt to a few hundred watts or even kilowatts.

2. Theoretical considerations

When a material is magnetized in an applied magnetic field, the entropy associated with the magnetic degrees of freedom, the so called magnetic entropy S_m, is changed as the field changes the magnetic order of the material. Under adiabatic conditions, ΔS_m must be compensated by an equal but opposite change of the entropy associated with the lattice, resulting in a change in temperature of the material. This temperature change, ΔT_{ad}, is usually called the MCE. It is related to the magnetic properties of the material through the thermodynamic Maxwell relation

$$\left(\frac{\partial S}{\partial B}\right)_T = \left(\frac{\partial M}{\partial T}\right)_B. \qquad (1)$$

For magnetization measurements made at discrete temperature intervals, ΔS_m can be calculated by means of

$$\Delta S_m(T, B) = \sum_i \frac{M_{i+1}(T_{i+1}, B) - M_i(T_i, B)}{T_{i+1} - T_i} \Delta B, \qquad (2)$$

where $M_{i+1}(T_{i+1}, B)$ and $M_i(T_i, B)$ represent the values of the magnetization in a magnetic field B at the temperatures T_{i+1} and T_i, respectively. On the other hand, the magnetic entropy change can be obtained more directly from a calorimetric measurement of the field dependence of the heat capacity and subsequent integration:

$$\Delta S_m(T, B) = \int_0^T \frac{C(T', B) - C(T', 0)}{T'} dT', \qquad (3)$$

where $C(T, B)$ and $C(T, 0)$ are the values of the heat capacity measured in a field B and in zero field, respectively. It has been confirmed that the values of $\Delta S_m(T, B)$ derived from the magnetization measurement coincide with the values from the calorimetric measurement [3, 4].

The adiabatic temperature change can be integrated numerically using the experimentally measured or theoretically predicted magnetization and heat capacity

$$\Delta T_{ad}(T, B) = -\int_0^B \frac{T}{C(T, B')} \left(\frac{\partial M}{\partial T}\right)_B dB'. \qquad (4)$$

Obviously, the MCE is large when $(\partial M/\partial T)_B$ is large, and $C(T, B)$ is small at the same temperature. This condition is true for paramagnetic materials near zero Kelvin where the magnetic susceptibility diverges, and the heat capacity approaches zero. This is the reason why the first realization of magnetic refrigeration worked at very low temperatures [5]. As we are interested in effects at higher temperatures, the heat capacity is generally quite large, of the order of the Dulong Petit rule; $C \sim 3NR$ with N the number of atoms and R the molar gas constant. Therefore, we should concentrate on finding a large change in magnetization at the relevant temperature. Since $(\partial M/\partial T)_B$ peaks at the magnetic ordering temperature, a large MCE is expected close to this magnetic phase-transition, and the effect may be further maximized, when the order-parameter of the phase transition changes strongly within a narrow temperature-interval. The latter is true for phase transitions of first order.

Most magnetic phase-transitions are of second order; there exist two theoretical models that under certain conditions account for first order phase-transition, the model of itinerant electron metamagnets and the Bean–Rodbell model [6, 7]. In the former, spin fluctuations are treated in a Landau–Ginzburg type of approach. Bean and Rodbell postulate a strong volume dependence of the critical temperature and find, for a certain range of parameters, a local minimum in the Gibb's free energy. These models are currently used to describe the unusual magnetic response of several possible magnetic refrigerants that will be discussed below.

In view of the applications the interest in first order transitions is directly related to the fact that a relatively small applied magnetic field can induce a strong change in entropy because it includes a certain amount of latent heat. However, with any first order transition, thermal- or field-hysteresis is also occurring which for applications should be small.

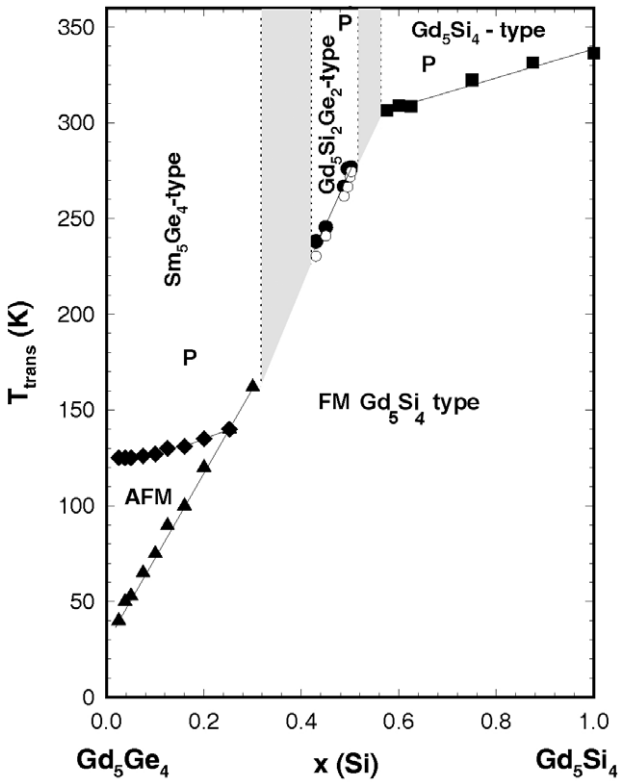

Figure 2. Low temperature part of the pseudo-binary phase-diagram Gd_5Ge_4–Gd_5Si_4 reprint from [12]. In the shaded regions phases co-exist.

3. $Gd_5(Ge,Si)_4$ and related compounds

Though the MCE was first discovered in simple iron [8], for years research on magnetocaloric materials was concentrated on rare-earth and their compounds. Following the discovery of a sub-room temperature giant-MCE in the ternary compound $Gd_5(Ge_{1-x}Si_x)_4$ ($0.3 \leqslant x \leqslant 0.5$) [9], there is a strongly increased interest from both fundamental and practical points of view to study the MCE in these materials [10, 11]. The most prominent feature of these compounds is that they undergo a first-order structural and magnetic phase transition, which leads to a giant magnetic field-induced entropy change, across their ordering temperature. Therefore we will discuss here to some extent the structural properties of these compounds. At low temperatures for all x $Gd_5(Ge_{1-x}Si_x)_4$ adopts an orthorhombic Gd_5Si_4-type structure (Pnma), and the ground state is ferromagnetic [12]. However, at room temperature depending on x three different crystallographic phases are observed. For $x > 0.55$ the aforementioned Gd_5Si_4 structure is stable, for $x < 0.3$ the materials adopt the Sm_5Ge_4-type structure with the same space group (Pnma) but a different atomic arrangement and a somewhat larger volume; finally, in between these two structure types the monoclinic $Gd_5Si_2Ge_2$ type with space group ($P112_1/a$) is formed, which has an intermediate volume. The latter structure type is stable only below about 570 K where again the orthorhombic Gd_5Si_4-type structure is formed in a first-order phase transition [13]. In figure 2 taken from Pecharsky *et al* [12] the low temperature phases are depicted; the shaded regions indicate two-phase regions. As one may guess, the three structure types are closely related; the unit cells contain four formula units and essentially only differ in the mutual arrangement of identical building blocks which are either connected by two, one or no covalent-like Si–Ge bonds, resulting in successively increasing unit-cell volumes. The giant MCE is observed for the compounds that exhibit a simultaneous paramagnetic to ferromagnetic, and structural phase-transition that can be either induced by a change in temperature, applied magnetic field or applied pressure [14, 15]. In contrast to most magnetic systems the ferromagnetic (FM) phase has a 0.4% smaller volume than the paramagnetic (PM) phase which results in an increase of T_c on application of pressure of about $3\,\mathrm{K\,kbar^{-1}}$. The structural change at the phase transition brings along also a very large magneto-elastic effect, and the electrical resistivity behaves anomalous. The strong coupling between lattice degrees of freedom and magnetic and electronic properties is rather unexpected, because the magnetic moment in Gd originates from spherical symmetric s-states that in contrast to other rare-earth elements hardly couple with the lattice. First principle electronic structure calculations in atomic sphere and local-density approximation with spin-orbit coupling added variationally could reproduce some distinct features of the phase transition [16]. Total energy calculations for the two phases show different temperature dependences, and the structural change occurs at the temperature where the energies are equal. There appears a distinct difference in the effective exchange-coupling parameter for the monoclinic and orthorhombic phase, respectively. This difference could be related directly to the change of the Fermi-level in the structural transition. Thus the fact that the structural and magnetic transitions are simultaneous is somewhat accidental as the exchange energy is of the same order of magnitude as the thermal energy at the structural phase-transition. The electrical resistivity and magneto resistance of $Gd_5Ge_2Si_2$ also shows unusual behaviour, indicating a strong coupling between electronic structure and lattice. For several compounds of the series, next to a cusp-like anomaly in the temperature dependence of the resistivity, a very large magnetoresistance effect is reported [17–20].

In view of building a refrigerator based on $Gd_5(Ge_{1-x}Si_x)_4$, there are a few points to consider. The largest MCE is observed at considerably below room temperature, while a real refrigerator should expel heat at least at about 320 K. Because the structural transition is connected with sliding of building blocks, impurities especially at the sliding interface can play an important role. The thermal hysteresis and the size of the MCE connected with the first-order phase transition strongly depend on the quality of the starting materials and the sample preparation [21]. For the compounds $Gd_5(Ge_{1-x}Si_x)_4$ with x around 0.5 small amounts of impurities may suppress the formation of the monoclinic structure near room temperature. These alloys then show only a phase transition of second order at somewhat higher temperature but with a lower MCE [13, 22, 23]. This sensitivity to impurities like carbon, oxygen and iron strongly influences the production costs of the materials which may hamper broad-scale application. Next to the thermal and field hysteresis the magneto-structural transition in $Gd_5(Ge_{1-x}Si_x)_4$ appears to be rather sluggish [24, 25]. This will also influence the optimal operation-frequency of a magnetic refrigerator and the efficiency.

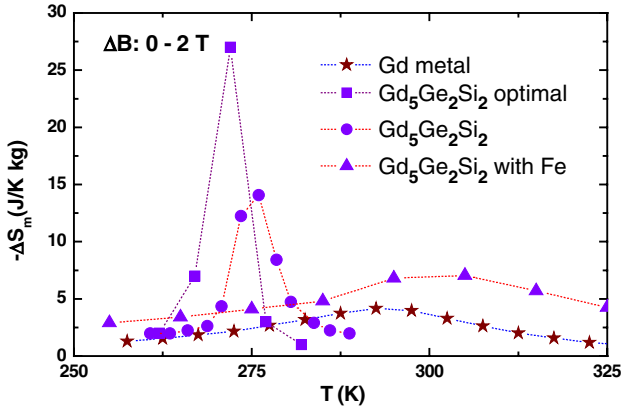

Figure 3. Magnetic-entropy change for different samples of $Gd_5Ge_2Si_2$ • [9] ■ [21] and $Gd_5Ge_{1.9}Si_2Fe_{0.1}$ ▲ [23] at a field change of 2 T.

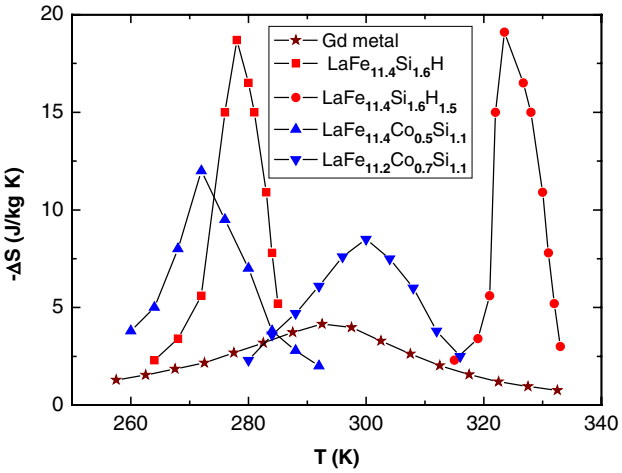

Figure 4. Magnetic-entropy change for different $LaFe_{13}$ based samples at a field change of 2 T [36, 47].

Other $R_5(Si,Ge)_4$ compounds are also found to form in the monoclinic $Gd_5Si_2Ge_2$ type structure, and when the structural transformation coincides with the magnetic ordering transition a large MCE is observed. This is most strikingly evidenced in the experiments of Morellon *et al* [26] on $Tb_5Si_2Ge_2$ where the two transitions were forced to coincide by the application of hydrostatic pressure, which results in a strong enhancement of the magnetic entropy change at the ordering temperature. The magnetic ordering temperatures of other $R_5(Si,Ge)_4$ compounds are all lower than for the Gd compound as expected. For cooling applications below liquid nitrogen temperatures some of these compounds may be interesting (figure 3).

4. La(Fe,Si)$_{13}$ and related compounds

Another interesting type of materials are rare-earth–transition-metal compounds crystallizing in the cubic $NaZn_{13}$ type of structure. $LaCo_{13}$ is the only binary compound, from the 45 possible combinations of a rare-earth and iron, cobalt or nickel, that exists in this structure. It has been shown that with an addition of at least 10% Si or Al this structure can also be stabilized with iron and nickel [27]. The $NaZn_{13}$ structure contains two different Zn sites. The Na atoms at 8a and Zn^{I} atoms at 8b form a simple CsCl type of structure. Each Zn^{I} atom is surrounded by an icosahedron of 12 Zn^{II} atoms at the 96i site. In La(Fe,Si)$_{13}$ La goes on the 8a site; the 8b site is fully occupied by Fe and the 96i site is shared by Fe and Si. The iron rich compounds La(Fe,Si)$_{13}$ show typical invar behaviour, with magnetic ordering temperatures around 200 K that increase to 262 K with lower iron content [28]. Thus, though the magnetic moment is diluted and also decreases per Fe atom, the magnetic ordering temperature increases. Around 200 K the magnetic-ordering transition is found to be also distinctly visible in the electrical resistivity, where a chromium-like cusp in the temperature dependence is observed. In contrast to $Gd_5Ge_2Si_2$ this phase-transition is not accompanied by a structural change; thus above and below T_c the material is cubic. Recently, because of the extremely sharp magnetic ordering transition, the (La,Fe,Si,Al) system was reinvestigated by several research groups, and a large MCE was reported [29–31]. The largest effects are observed for the compounds that show a field- or temperature-induced phase-transition of first order. Unfortunately, these large effects only occur up to about 210 K as the magnetic sublattice becomes more and more diluted. When using standard melting techniques, the preparation of homogeneous single-phase samples appears to be rather difficult especially for alloys with high transition metal content. Almost single phase samples are reported when, instead of normal arc melting, rapid quenching by melt spinning and subsequent annealing is employed [32–34]. Samples prepared in this way also show a very large MCE. To increase the magnetic ordering temperature without losing too much magnetic moment, one may replace some Fe by other magnetic transition-metals. Because the isostructural compound $LaCo_{13}$ has a very high critical temperature substitution of Co for Fe is widely studied. The compounds $La(Fe,Co)_{13-x}Al_x$ and $La(Fe,Co)_{13-x}Si_x$ with $x \approx 1.1$ and thus a very high transition-metal content show a considerable MCE near room temperature [35–38]. This is achieved with only a few per cent of Co, and the Co content can easily be varied to tune the critical temperature to the desired value. It should be mentioned however that near room temperature the values for the entropy change steeply drop (figure 4).

The fact that the alloys with the highest Fe content have an antiferromagnetic ground-state indicates that antiferromagnetic direct exchange-interaction plays an important role in these compounds. Taking into account that this occurs at a very high Fe density, one may expect that expansion of the lattice will lead to an increase in ferromagnetic exchange. In rare-earth transition-metal compounds this can be achieved by hydrogenation, or introduction of other small atoms like B, C or N. A very strong lattice expansion (<9%) and increase of T_c to almost 900 K is observed when nitrogen is used as interstitial element in La(Fe, Al)$_{13}$ [39]. Alloys with low aluminium content are found to accommodate up to 3 nitrogen atoms per formula unit. However, careful structural analysis showed that the interstitial atoms are located at 24d sites between the icosahedrons formed by Fe^{II}; thus the Fe–Fe separation hardly changes, and the strong increase in T_c should rather be attributed to changes in the electronic structure than to changes in interatomic distances [40, 41]. The effect of

interstitial nitrogen on the magnetocaloric properties has not been studied yet. One may however expect that it is considerably reduced because the magnetic moments are reduced, and the phase transition appears to be broadened. The latter however can be due to the fact that most samples studied so far are not fully homogeneous. Finally it should be mentioned that the authors of all studies on nitrogenated samples report the occurrence of considerable amounts of α Fe as impurity phase. Carbon as interstitial atom also leads to an increase in critical temperature [42–46]. Similarly to the nitrogen interstitials the Fe magnetic moments are reduced, and for 0.5 carbon atoms per formula unit the phase transition becomes of second order with a much lower magnetic entropy change.

Hydrogen is the most promising interstitial element. In contrast to the above mentioned interstitial atoms, interstitial hydrogen not only increases the critical temperature but also leads to an increase in magnetic moment [30, 47–51]. The lattice expansion due to the addition of three hydrogen atoms per formula unit is about 4.5%. The critical temperature can be increased to up to 450 K; the average magnetic moment per Fe increases from 2.0 μ_B to up to 2.2 μ_B, and the field- or temperature-induced phase-transition is found to be of first-order for all hydrogen concentrations. All this results for a certain Si percentage in an almost constant value of the magnetic entropy change per mass unit over a broad temperature span, see the hydrides in figure 4.

Obviously the question arises as to what causes the distinct differences resulting from different interstitial elements. The lower lattice expansion observed for hydrogen is consistent with the smaller volume of hydrogen compared with carbon or nitrogen. Unfortunately there are no electronic band-structure calculations available for these compounds, but from general arguments we may discuss the observations. The lattice expansion, common to all interstitial alloys, leads to a narrowing of the Fe d-states and thus results in an increase in critical temperature and moment. On the other hand Fe d-states may hybridize stronger with C- or N p-states than with H s-states, and it is well known that hybridization leads to a reduced moment [52] and thus lead C and N interstitials to a net loss of moment. Because the interstitial sites are surrounded by a large fraction of Fe this effect is stronger than the former increase and thus leads C and N interstitials to a net loss of moment. However, concerning the position of the interstitials, one would then expect that the reduction in moment would be stronger at Fe^{II} sites rather than at Fe^{I} sites, which is opposite to the observations from neutron diffraction [40]. Obviously the interplay of exchange interaction and moment formation is more complex in these materials.

From the materials cost point of view the $La(Fe,Si)_{13}$ type of alloys appear to be very attractive. La is the cheapest of the rare-earth series, and both Fe and Si are available in large amounts. The processing will be a little more elaborate than for a simple metal alloy, but this can be optimized. For use in a magnetic refrigerator next to the magnetocaloric properties mechanical properties and chemical stability may also be of importance. The hydrogenation process of rare-earth transition-metal compounds always produces granular material due to the strong lattice expansion. In the case of the cubic $NaZn_{13}$ type of structure this does not seem to be the case. At the phase transition in $La(Fe,Si)_{13}$ type of alloys a volume change of 1.5% is also observed [53]. If this volume change is performed very frequently the material will definitely become very brittle and probably break into even smaller grains. This can have a distinct influence on the corrosion resistance of the material and thus on the lifetime of a refrigerator. The suitability of this material definitely needs to be tested.

5. MnAs based compounds

MnAs exists similar to $Gd_5Ge_2Si_2$ in two distinct crystallographic structures [54]. At low and high temperature the hexagonal NiAs structure is found, and for a narrow temperature range 307–393 K the orthorhombic MnP structure exists. The high temperature transition in the paramagnetic region is of second order. The low temperature transition is a combined structural and ferro-paramagnetic transition of first order with large thermal hysteresis. The change in volume at this transition amounts to 2.2% [55]. The transition from paramagnetic to ferromagnetic occurs at 307 K and the reverse transition from ferromagnetic to paramagnetic occurs at 317 K. Very large magnetic entropy changes are observed in this transition [56, 57]. Similarly to the application of pressure [58, 59] substitution of Sb for As leads to a lowering of T_c [60, 61]; 25% of Sb gives a transition temperature of 225 K. However, the thermal hysteresis is affected quite differently by hydrostatic pressure or Sb substitution. In Mn(As,Sb) the hysteresis is strongly reduced, and at 5% Sb it is reduced to about 1 K. In the concentration range 5–40% of Sb T_C can be tuned between 220 and 320 K without losing much of the magnetic entropy change [62, 63]. Direct measurements of the temperature change confirm a ΔT of 2 K T^{-1} [64]. On the other hand MnAs under pressure shows an extremely large magnetic entropy change [65] in conjunction with large hysteresis.

The materials costs of MnAs are quite low; processing of As containing alloys is however complicated due to the biological activity of As. In the MnAs alloy the As is covalently bound to the Mn and would not be easily released into the environment. However, this should be experimentally verified, especially because in an alloy second phases frequently form that may be less stable. The change in volume in Mn(As,Sb) is still 0.7%, which may result in ageing after frequent cycling of the material.

6. Heusler alloys

Heusler alloys frequently undergo a martensitic transition between the martensitic and the austenitic phase, which is generally temperature induced and of first order. Ni_2MnGa orders ferromagnetic with a Curie temperature of 376 K, and a magnetic moment of 4.17 μ_B, which is largely confined to the Mn atoms and with a small moment of about 0.3 μ_B associated with the Ni atoms [66]. As may be expected from its cubic structure, the parent phase has a low magneto-crystalline anisotropy energy ($H_a = 0.15$ T). However, in its martensitic phase the compound is exhibiting a much larger anisotropy ($H_a = 0.8$ T). The martensitic-transformation temperature is near 220 K. This martensitic transformation temperature can be easily varied to around room temperature by modifying the composition of the alloy from the stoichiometric one. The low-temperature phase evolves from the parent phase by a

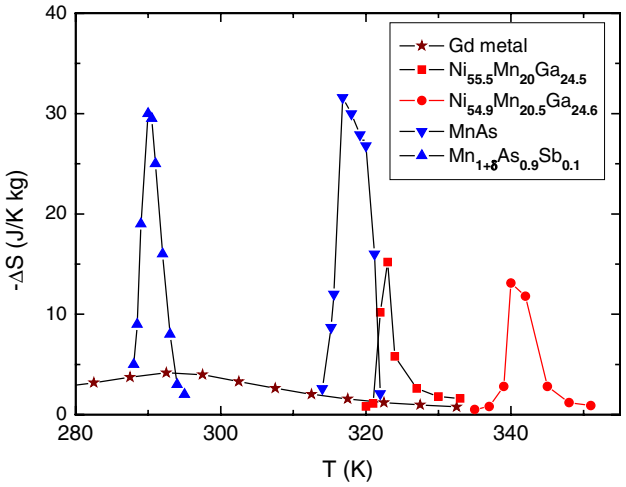

Figure 5. Magnetic-entropy change for MnAs and $Mn_{1+\delta}As_{0.9}Sb_{0.1}$ [62] and two NiMnGa [71] alloys at a field change of 2 T.

diffusionless, displacive transformation leading to a tetragonal structure, $a = b = 5.90$ Å, $c = 5.44$ Å. A martensitic phase generally accommodates the strain associated with the transformation (this is 6.56% along c for Ni_2MnGa) by the formation of twin variants. This means that a cubic crystallite splits up into two tetragonal crystallites sharing one contact plane. These twins pack together in compatible orientations to minimize the strain energy (much the same as the magnetization of a ferromagnet may take on different orientations by breaking up into domains to minimize the magneto-static energy). Alignment of these twin variants by the motion of twin boundaries can result in large macroscopic strains. In the tetragonal phase with its much higher magnetic anisotropy, an applied magnetic field can induce a change in strain, which is why these materials may be used as actuators. Next to this ferromagnetic shape memory effect, very close to the martensitic transition temperature, one observes a large change in magnetization for low applied magnetic fields. This change in magnetization is also related to the magnetocrystalline anisotropy. This change in magnetization results in a moderate magnetic entropy change of a few J/mol K, which is enhanced when measured on a single crystal [67,68]. When the composition in this material is tuned in a way that the magnetic and structural transformation occurs at the same temperature, the largest magnetic entropy changes are observed [69–71] (figure 5).

For magnetocaloric applications the extremely large length changes in the martensitic transition will definitely result in ageing effects. It is well known for the magnetic shape-memory alloys that only single crystals can be frequently cycled while polycrystalline materials spontaneously powderize after several cycles.

7. Fe_2P based compounds

The binary intermetallic compound Fe_2P can be considered the parent alloy for an interesting type of materials. This compound crystallizes in the hexagonal non-centre-symmetric Fe_2P type structure with space group $P\bar{6}2m$. In this structure Fe and P occupy four different crystallographic sites, Fe occupies the 3g and 3f sites and P the 1b and 2c sites. Thus one has a stacking of alternating P-rich and P-poor layers. Neutron diffraction revealed that the magnetic moment of Fe on the 3g sites is about 2 μ_B whereas the moment on the 3f sites is about 1 μ_B [72]. The Curie temperature of this compound is 216 K, and the magnetic transition is of first order [73]. The magnetic-ordering transition from the paramagnetic state to the ferromagnetic state is accompanied by a discontinuous change of the volume of 0.05%. Thus, the ferromagnetic state has a higher volume than the paramagnetic one. This phase transition is found to be extremely sensitive to changes in pressure or magnetic field. Application of pressure first reduces the Curie temperature, and at pressures exceeding 5 kbar antiferromagnetic ordering preceding the ferromagnetic ordering is observed [74]. Substitution of As, B or Si into the P sublattice results in an increase of the Curie temperature [75], which can easily be lifted to above room temperature for As or Si concentrations of 10% or by 4% of B. Substitution of Mn for Fe on the 3g sites further increases the magnetic moment to about 4 μ_B. To stabilize the Fe_2P-type of structure, simultaneously with the Mn substitution part of the P should also be replaced.

The most extensively studied series of alloys is of the type MnFe(P,As). The magnetic phase diagram for the system MnFeP–MnFeAs [76] shows a rich variety of crystallographic and magnetic phases. The most striking feature is the fact that for As concentrations between 30% and 65% the hexagonal Fe_2P type of structure is stable, and the ferromagnetic order is accompanied by a discontinuous change of volume. While the total magnetic moment is not affected by changes of the composition, the Curie temperature increases from about 150 K to well above room temperature. We reinvestigated this part of the phase diagram [77, 78] and investigated the possibilities of partially replacing the As [79–81].

Polycrystalline samples can be synthesized starting from the binary Fe_2P and $FeAs_2$ compounds, Mn chips and P powder (red) mixed in the appropriate proportions by ball milling under a protective atmosphere. After this mechanical alloying process one obtains an amorphous powder. To obtain dense material of the crystalline phase, the powders are pressed into pellets wrapped in Mo foil and sealed in quartz tubes under an argon atmosphere. These are heated at 1273 K for 1 h, followed by a homogenization process at 923 K for 50 h and finally by slow cooling to ambient conditions. The powder x-ray diffraction patterns show that the compound crystallizes in the hexagonal Fe_2P type structure. In this structure the Mn atoms occupy the 3g sites, the Fe atoms occupy the 3f sites and the P and the As atoms occupy 2c and 1b sites statistically [82]. From the broadening of the x-ray diffraction reflections, the average grain size is estimated to be about 100 nm [83].

Figure 6 shows the change in critical temperature on the application of a magnetic field. As pointed out in [84], this change in critical temperature is a good indication for the temperature change induced by the application of a magnetic field. The inset of figure 6 shows the temperature dependence of the magnetization near room temperature of $MnFeP_{0.45}As_{0.55}$ and Gd (Alfa Aesar 3N) as determined in an applied magnetic field of 1 T. It is obvious that the change in magnetization in $(Mn,Fe)_2(P,As)$ compounds at the ordering

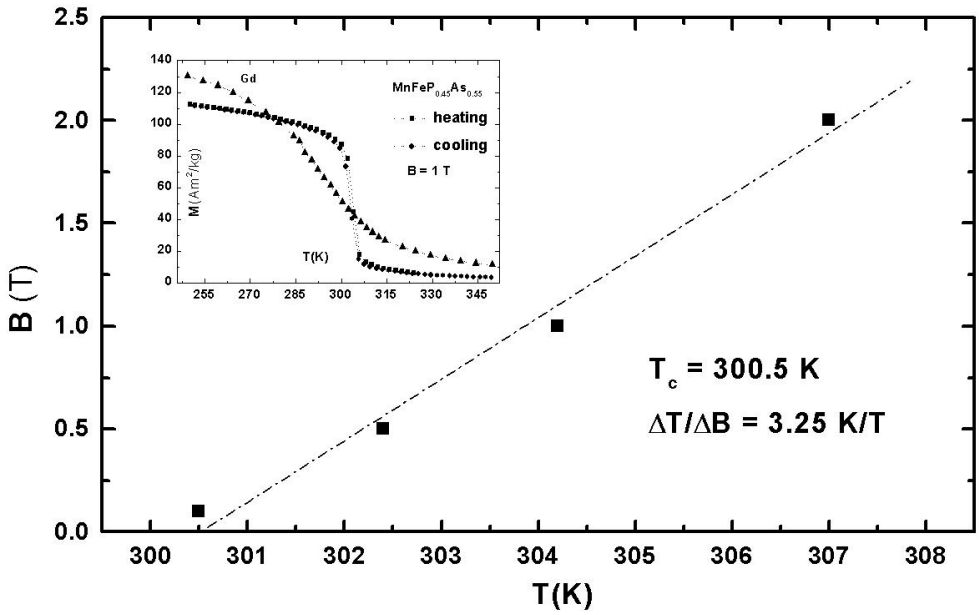

Figure 6. Variation of critical temperature with applied magnetic field; the line is a least square fit of the data. Inset: temperature dependence of the magnetization for $MnFeP_{0.45}As_{0.55}$ and Gd measured with increasing (heating) and decreasing (cooling) temperature in a field of 1 T.

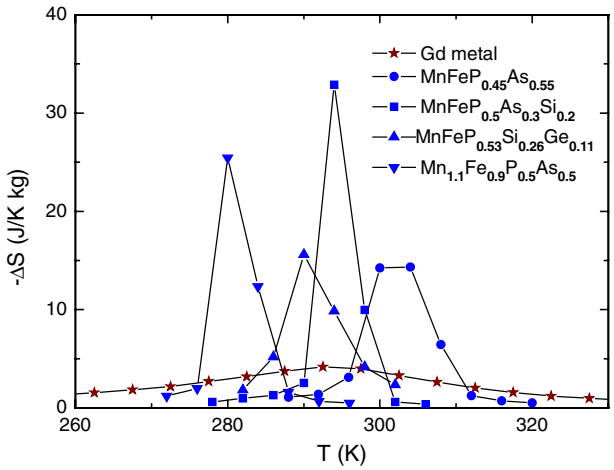

Figure 7. Magnetic-entropy changes of Fe_2P type compounds at magnetic field changes of 2 T [83, 85, 86, 90].

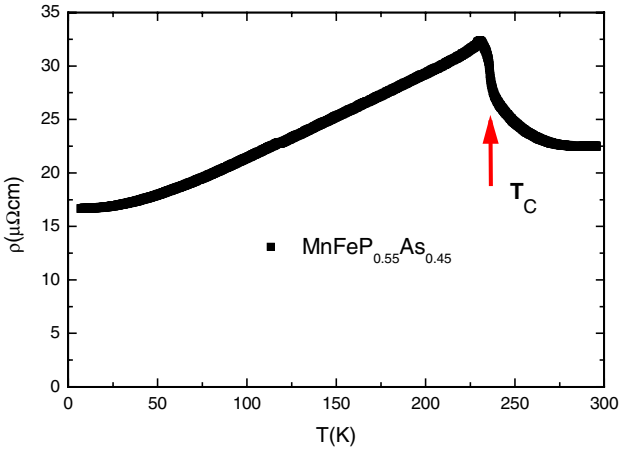

Figure 8. Temperature dependence of the electrical resistivity of $MnFeP_{0.55}As_{0.45}$, measured with decreasing temperature. T_C is at the maximum of the temperature derivative.

temperature T_c is much larger, despite the fact that the magnetic moment of Gd is much larger at low temperatures 248 $Am^2\,kg^{-1}$ compared with 125 $Am^2\,kg^{-1}$. Variation of the P/As ratio between 3/2 and 1/2 makes it possible to tune T_c and the optimal operating temperature between 200 and 350 K (−70 and 80 °C), without losing the large MCE. The inset shows the temperature dependence of the magnetization measured with increasing and decreasing temperature in an applied field of 1 T. The thermal hysteresis is the signature of a first-order phase transition. Because of the small size of the thermal hysteresis (less than 1 K), the magnetization process can be considered as being reversible in temperature. From the magnetization curve at 5 K, the saturation magnetization was determined as 3.9 μ_B/f.u. This high magnetization originates from the parallel alignment of the Mn and Fe moments, though the moments of Mn are much larger than those of Fe [76]. Variation of the Mn/Fe ratio may also be used to further improve the MCE. Recently, we have observed a surprisingly large MCE in the compound $MnFeP_{0.5}As_{0.3}Si_{0.2}$ at room temperature [85]. After replacing all As a considerably large MCE is still observed for MnFe(P,Si,Ge) [86].

We calculate the magnetic-entropy changes, ΔS_m, from magnetization data by means of equation (2). The results for several compounds are shown in figure 7. The calculated maximum values of the magnetic entropy change are 14.5, 25.4 and 32.9 $J\,kg^{-1}K^{-1}$ for a field change from 0 to 2 T. The maximum magnetic entropy in 3d materials depends on the spin moment S. Because there are two magnetic ions per formula unit, one has $S_m = 2R\ln(2S+1)$, where R is the universal gas constant. From the saturation magnetic moment, we estimate the average S value of the magnetic ions to be equal to $S = 1$ thus $S_m = 18.3\,J\,mol^{-1}\,K^{-1} = 117\,J\,kg^{-1}K^{-1}$, which is about 3.5 times larger than the value obtained from the magnetization measurements. For comparison, the

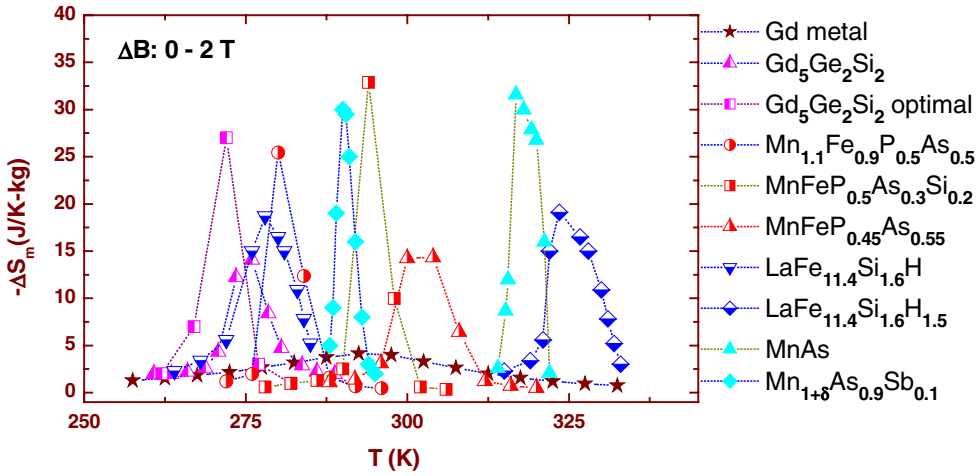

Figure 9. Magnetic entropy-change of different materials at magnetic field changes of 2 T.

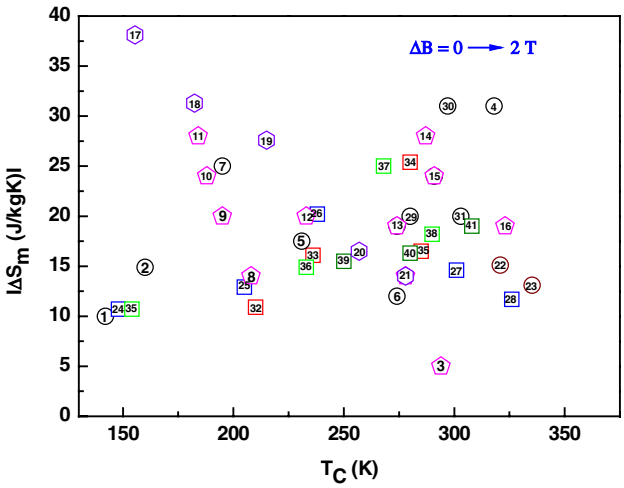

Figure 10. Maximal observed entropy-change of various materials at magnetic field changes of 2 T. 1 $DyCo_2$ [91], 2 Mn_3GaC [92], 3 Gd [93], 4 MnAs [60], 5 $MnAs_{0.75}Sb_{0.25}$ [60], 6 $LaFe_{11.2}Co_{0.7}Si_{1.1}$ [94], 7 $LaFe_{11.8}Si_{1.2}$ (melt-spun) [34], 8 $La(Fe_{0.877}Si_{0.123})_{13}$ [47], 9 $La(Fe_{0.880}Si_{0.120})_{13}$ [47], 10 $La(Fe_{0.890}Si_{0.110})_{13}$ [47], 11 $La(Fe_{0.90}Si_{0.10})_{13}$ [47], 12 $La(Fe_{0.88}Si_{0.12})_{13}H_{0.5}$ [47], 13 $La(Fe_{0.88}Si_{0.12})_{13}H_{1.0}$ [47], 14 $LaFe_{11.7}Si_{1.3}H_{1.1}$ [47], 15 $LaFe_{11.57}Si_{1.43}H_{1.3}$ [47], 16 $La(Fe_{0.88}Si_{0.12})H_{1.5}$ [47], 17 $Gd_5(Si_{0.25}Ge_{0.75})_4$ [95], 18 $Gd_5(Si_{0.30}Ge_{0.70})_4$ [95], 19 $Gd_5(Si_{0.365}Ge_{0.635})_4$ [95], 20 $Gd_5(Si_{0.45}Ge_{0.55})_4$ [95], 21 $Gd_5(Si_{0.45}Ge_{0.55})_4$ [95], 22 $Ni_{55.5}Mn_{20}Ga_{24.5}$ [71], 23 $Ni_{54.9}Mn_{20.5}Ga_{24.6}$ [71], 24 $MnFeP_{0.75}As_{0.25}$ [78], 25 $MnFeP_{0.65}As_{0.35}$ [78], 26 $MnFeP_{0.55}As_{0.45}$ [78], 27 $MnFeP_{0.45}As_{0.55}$ [78], 28 $MnFeP_{0.35}As_{0.65}$ [78], 29 $MnFeP_{0.5}As_{0.4}Si_{0.1}$ [85], 30 $MnFeP_{0.5}As_{0.3}Si_{0.2}$ [85], 31 $MnFeP_{0.5}As_{0.2}Si_{0.3}$ [85], 32 $Mn_{1.3}Fe_{0.7}P_{0.5}As_{0.5}$ [77], 33 $Mn_{1.2}Fe_{0.8}P_{0.5}As_{0.5}$ [77], 34 $Mn_{1.1}Fe_{0.9}P_{0.5}As_{0.5}$ [77], 35 $Mn_{1.1}Fe_{0.9}P_{0.7}As_{0.3}$ [77], 36 $Mn_{1.1}Fe_{0.9}P_{0.7}As_{0.25}Ge_{0.05}$ [80], 37 $Mn_{1.1}Fe_{0.9}P_{0.7}As_{0.2}Ge_{0.1}$ [80], 38 $Mn_{1.1}Fe_{0.9}P_{0.7}As_{0.15}Ge_{0.15}$ [80], 39 $Mn_{1.1}Fe_{0.9}P_{0.80}Ge_{0.20}$ [96], 40 $Mn_{1.1}Fe_{0.9}P_{0.78}Ge_{0.22}$ [96], 41 $Mn_{1.1}Fe_{0.9}P_{0.77}Ge_{0.23}$ [96].

magnetic-entropy change of Gd is also shown in figure 7. The origin of the large magnetic-entropy change should be attributed to the comparatively high 3d moments and the rapid change of the magnetization in the field-induced magnetic phase transition. In rare-earth materials, the magnetic moment fully develops only at low temperatures, and therefore the entropy change near room temperature is only a fraction of their potential. In 3d compounds, the strong magneto-crystalline coupling results in competing intra- and inter-atomic interactions and leads to a modification of metal–metal distances which may change the iron and manganese magnetic moment and favours the spin ordering.

Bearing in mind the use of these materials in magnetic refrigerators, next to the magnetocaloric properties the electrical and heat conductivity is also of utmost importance. There is hardly any information on the electrical-transport properties of these alloys. The electrical resistance can also be useful for a more detailed investigation of the magnetic phase transition because it is very sensitive to changes in the interactions between magnetic ions. The availability of electrical-resistance data would make it possible to compare the critical magnetic fields derived from magnetic and electrical measurements and to understand the role of the electron–phonon and electron–magnon interactions in the magnetic phase transitions. The temperature dependence of the electrical resistance of $MnFeP_{0.55}As_{0.45,}$ measured during the cooling of a sample of $MnFeP_{0.55}As_{0.45}$, is presented in figure 8. It can be seen that there is an anomaly in the temperature dependence of the electrical resistance at $T_{cr} = 231$ K. Below T_{cr}, the electrical resistance increases with increasing temperature and has metallic character but, above T_{cr}, it decreases dramatically in a narrow temperature range and then recovers the metal-like dependence on temperature. The total contribution from both the electron–phonon scattering and the electron–magnon scattering in the PM is smaller than in the FM which is contrary to normal ferromagnetic metallic materials. It is interesting to note that the transition at T_{cr} is accompanied by a change in the c/a ratio [76], which may lead to a change in the Fermi-surface topology and may affect the electron–phonon scattering. Preliminary band-structure calculations indicate a strong shift of the Fermi level associated with the phase-transition [87].

The large MCE observed in Fe_2P based compounds originates from a field-induced first-order magnetic phase transition. The magnetization is reversible in temperature and in alternating magnetic field. The magnetic ordering

Table 1. Comparison of different potential magnetocaloric materials. Gd is included as reference material.

Material	T range K	ΔS_{max} (2 T) J kg^{-1} K^{-1}	ΔT (2 T) K	T_C K	Costs €/kg	Density 10^3 kg m^{-3}	Reference
Gd	270–310	5	5.8[d]	293	20	7.9	[3]
$Gd_5Ge_2Si_2$	150–290	27	6.6[d]	272	60	7.5	[21, 25]
La(Fe,Si)H	180–320	19	7[c]	300	8	7.1	[47]
MnAs	220–320	32	4.1[d]	287	10	6.8	[62, 64]
MnNiGa	310–350	15	2[c]	317	10	8.2	[71]
MnFe(P,As)	150–450	32	6[d]	292	7	7.3	[89]

[d] means direct measurement [c] is calculated from a combination of measurements.
Note: The costs may strongly fluctuate due to market demands and quality of starting materials.

temperature of these compounds is tuneable over a wide temperature interval (200–450 K). The excellent magnetocaloric features of the compounds of the type MnFe(P,Si,Ge,As), in addition to the very low material costs, make it an attractive candidate material for a commercial magnetic refrigerator. However as for MnAs alloys it should be verified that materials containing As do not release this into the environment. The fact that the magneto-elastic phase-transition is rather a change of c/a than a change of volume makes it feasible that this alloy even in polycrystalline form will not experience severe ageing effects after frequent magnetic cycling.

8. Comparison of different materials and outlook

The MCEs for field changes of 2 T are summarized in figures 9 and 10. It is obvious that above room temperature a few transition-metal-based alloys perform the best. If one takes into account the fact that ΔT also depends on the specific heat of the compound [88] these alloys are still favourable, and not only from the cost point of view. This makes them likely candidates for use as magnetic refrigerant materials above room temperature. However, below room temperature a number of rare-earth compounds perform better, and for these materials a thorough cost versus performance analysis will be needed.

The main parameters of the various materials are also summarized in table 1 which allows a fast comparison. At present it is not clear which material will really get to the stage of real life applications. Though it is already feasible that for applications with limited temperature span and a cooling power in the kilowatt range like air conditioning, commercial competitive magnetic refrigerators are quite possible, it is not yet obvious which of the above mentioned materials shall be employed. Currently most attention is paid to the pure magnetocaloric properties and materials costs. In the near future also other properties like corrosion resistance, mechanical properties, heat conductivity, electrical resistivity and environmental impact should be addressed.

Taking into account the different requirements for magnetic refrigerants, it may be stated that the ideal magnetic refrigerant should at least contain 80% transition metals with a large magnetic moment like Fe or Mn. In addition to this it should contain some cheap p-metal like Al or Si that can be used to tune the working point of the material. This material should then exhibit a magnetic ordering-transition of first order, be workable as steel, with a corrosion resistance like stainless steel and a high electrical resistance. From that point of view one may get the impression that magnetic refrigeration will experience a similar future as fuel cells in the past 20 years. However, magnetic refrigeration is already currently much further developed. The gap with market is less severe, because the refrigerators and heat pumps will consist of mainly the same parts as today's technology except for the compressor. At the first Conference on Magnetic Refrigeration near Room Temperature held in Montreux, September 2005, Steve Russek from Astronatics Co., Milwaukee, WI, stated 'provided enough magnetocaloric materials are produced, a competing magnetic heat-pump could be on the market within one year'.

Acknowledgments

Special thanks are due to Vitalij Pecharsky for providing figure 2 and to O Tegus for figures 9 and 10. This work is supported by the Dutch Technology Foundation STW, Applied Science Division of NWO and the Technology Program of the Ministry of Economic Affairs.

References

[1] Zimm C, Jastrab A, Sternberg A, Pecharsky V and Geschneidner K Jr 1998 *Adv. Cryog. Eng.* **43** 1759–66
[2] Tishin A M 1999 *Handbook of Magnetic Materials* vol 12, ed K H J Buschow (Amsterdam: North Holland) pp 395–524
[3] Gschneidner K A, Pecharsky V K, Pecharsky A O and Zimm C B 1999 *Rare Earths '98* vol 315–3, pp 69–76
[4] Tegus O, Duong N P, Dagula W, Zhang L, Brück E, Buschow K H J and de Boer F R 2002 *J. Appl. Phys.* **91** 8528–30
[5] Giauque W F and MacDougall D P 1933 *Phys. Rev.* **43** 768
[6] Bean C P and Rodbell D S 1962 *Phys. Rev.* **126** 104–15
[7] Moriya T and Usami K 1977 *Solid State Commun.* **23** 935–40
[8] Warburg E 1881 *Ann. Phys. (Leipzig)* **13** 141
[9] Pecharsky V K and Gschneidner K A 1997 *Phys. Rev. Lett.* **78** 4494–7
[10] Choe W, Pecharsky V K, Pecharsky A O, Gschneidner K A, Young V G and Miller G J 2000 *Phys. Rev. Lett.* **84** 4617–20
[11] Morellon L, Blasco J, Algarabel P A and Ibarra M R 2000 *Phys. Rev.* B **62** 1022–6
[12] Pecharsky A O, Gschneidner K A, Pecharsky V K and Schindler C E 2002 *J. Alloys Compounds* **338** 126–35
[13] Mozharivskyj Y, Pecharsky A O, Pecharsky V K and Miller G J 2005 *J. Am. Chem. Soc.* **127** 317–24
[14] Morellon L, Algarabel P A, Ibarra M R, Blasco J, Garcia-Landa B, Arnold Z and Albertini F 1998 *Phys. Rev.* B **58** R14721–4
[15] Morellon L, Arnold Z, Algarabel P A, Magen C, Ibarra M R and Skorokhod Y 2004 *J. Phys. Condens. Matter* **16** 1623–30

[16] Pecharsky V K, Samolyuk G D, Antropov V P, Pecharsky A O and Gschneidner K A 2003 *J. Solid State Chem.* **171** 57–68

[17] Morellon L, Algarabel P A, Magen C and Ibarra M R 2001 *J. Magn. Magn. Mater.* **237** 119–23

[18] Levin E M, Pecharsky V K, Gschneidner K A and Miller G J 2001 *Phys. Rev.* B **64** 235103

[19] Tang H, Pecharsky V K, Samolyuk G D, Zou M, Gschneidner K A, Antropov V P, Schlagel D L and Lograsso T A 2004 *Phys. Rev. Lett.* **93** 237203

[20] Morellon L, Stankiewicz J, Garcia-Landa B, Algarabel P A and Ibarra M R 1998 *Appl. Phys. Lett.* **73** 3462–4

[21] Pecharsky A O, Gschneidner K A and Pecharsky V K 2003 *J. Appl. Phys.* **93** 4722–8

[22] Pecharsky V K and Gschneidner K A 1997 *J. Magn. Magn. Mater.* **167** L179–84

[23] Provenzano V, Shapiro A J and Shull R D 2004 *Nature* **429** 853–7

[24] Giguere A, Foldeaki M, Gopal B R, Chahine R, Bose T K, Frydman A and Barclay J A 1999 *Phys. Rev. Lett.* **83** 2262–5

[25] Gschneidner K A, Pecharsky V K, Brück E, Duijn H G M and Levin E M 2000 *Phys. Rev. Lett.* **85** 4190

[26] Morellon L, Arnold Z, Magen C, Ritter C, Prokhnenko O, Skorokhod Y, Algarabel P A, Ibarra M R and Kamarad J 2004 *Phys. Rev. Lett.* **93** 159901

[27] Kripyakevich P I, Zarechnyuk O S, Gladyshevsky E I and Bodak O I 1968 *Z. Anorg. Chem.* **358** 90

[28] Palstra T T M, Mydosh J A, Nieuwenhuys G J, van der Kraan A M and Buschow K H J 1983 *J. Magn. Magn. Mater.* **36** 290–6

[29] Hu F X, Shen B G, Sun J R and Zhang X X 2000 *Chin. Phys.* **9** 550–3

[30] Fujieda S, Fujita A and Fukamichi K 2002 *Appl. Phys. Lett.* **81** 1276–8

[31] Hu F X, Shen B G, Sun J R, Pakhomov A B, Wong C Y, Zhang X X, Zhang S Y, Wang G J and Cheng Z H 2001 *IEEE Trans. Magn.* **37** 2328–30

[32] Liu X B, Altounian Z and Tu G H 2004 *J. Phys. Condens. Matter* **16** 8043–51

[33] Liu X B, Liu X D, Altounian Z and Tu G H 2005 *J. Alloys Compounds* **397** 120–5

[34] Gutfleisch O, Yan A and Muller K H 2005 *J. Appl. Phys.* **97** 10M305

[35] Hu F X, Shen B G, Sun J R and Cheng Z H 2001 *Phys. Rev.* B **64** 012409

[36] Hu F X, Gao J, Qian X L, Ilyn M, Tishin A M, Sun J R and Shen B G 2005 *J. Appl. Phys.* **97** 10M303

[37] Proveti J R, Passamani E C, Larica C, Gomes A M, Takeuchi A Y and Massioli A 2005 *J. Phys. D: Appl. Phys.* **38** 1531–9

[38] Shen J, Li Y X, Wang F, Wang G J and Zhang S Y 2004 *Chin. Phys.* **13** 1134–8

[39] Liu J P, Tang N, de Boer F R, de Chatel P F and Buschow K H J 1995 *J. Magn. Magn. Mater.* **140–144** 1035–6

[40] Moze O, Kockelmann W, Liu J P, de Boer F R and Buschow K H J 2000 *J. Appl. Phys.* **87** 5284–6

[41] Moze O, Kockelmann W, Liu J P, de Boer F R and Buschow K H J 1999 *J. Magn. Magn. Mater.* **195** 391–5

[42] Liu X B, Altounian Z and Ryan D H 2004 *J. Phys. D: Appl. Phys.* **37** 2469–74

[43] Shcherbakova Y V, Ivanova G V, Gaviko V S and Gabay A M 2003 *J. Magn. Magn. Mater.* **267** 26–34

[44] Liu X B, Altounian Z and Beath A D 2004 *J. Appl. Phys.* **95** 7067–9

[45] Chen Y F, Wang F, Shen B G, Sun J R, Wang G J, Hu F X, Cheng Z H and Zhu T 2003 *J. Appl. Phys.* **93** 6981–3

[46] Wang F, Chen Y F, Wang G J, Sun J R and Shen B G 2004 *J. Phys. Condens. Matter* **16** 2103–8

[47] Fujita A, Fujieda S, Hasegawa Y and Fukamichi K 2003 *Phys. Rev.* B **67** 104416

[48] Irisawa K, Fujita A, Fukamichi K, Yamazaki Y, Iijima Y and Matsubara E 2001 *J. Alloys Compounds* **316** 70–4

[49] Fujieda S, Fujita A and Fukamichi K 2004 *Mater. Trans.* **45** 3228–31

[50] Mandal K, Gutfleisch O, Yan A, Handstein A and Muller K H 2005 *J. Magn. Magn. Mater.* **290** 673–5

[51] Nikitin S A, Tereshina I S, Verbetsky V N, Salamova A A and Anosova E V 2004 *J. Alloys Compounds* **367** 266–9

[52] Qi Q N, Odonnell K, Touchais E and Coey J M D 1994 *Hyperfine Interact.* **94** 2067–73

[53] Wang F W, Wang G J, Hu F X, Kurbakov A, Shen B G and Cheng Z H 2003 *J. Phys. Condens. Matter* **15** 5269–78

[54] Pytlik L and Zieba A 1985 *J. Magn. Magn. Mater.* **51** 199–210

[55] Fjellvag H and K A 1984 *Acta Chem. Scand.* A **38** 1

[56] Wada H and Tanabe Y 2001 *Appl. Phys. Lett.* **79** 3302–4

[57] Kuhrt C, Schittny T and Barner K 1985 *Phys. Status Solidi* a **91** 105–13

[58] Menyuk N, Kafalas J A, Dwight K and Goodenough J B 1969 *Phys. Rev.* **177** 942

[59] Yamada H, Terao K, Kondo K and Goto T 2002 *J. Phys. Condens. Matter* **14** 11785–94

[60] Wada H, Morikawa T, Taniguchi K, Shibata T, Yamada Y and Akishige Y 2003 *Physica B: Condens. Matter* **328** 114–6

[61] Wada H, Taniguchi K and Tanabe Y 2002 *Mater. Trans.* **43** 73–7

[62] Wada H and Asano T 2005 *J. Magn. Magn. Mater.* **290** 703–5

[63] Morikawa T, Wada H, Kogure R and Hirosawa S 2004 *J. Magn. Magn. Mater.* **283** 322–8

[64] Wada H, Funaba C, Asano T, Ilyn M and Tishin A M 2005 *Sci. Tech. Froid C. R.* **2005–4** 37–46

[65] Gama S, Coelho A A, de Campos A, Carvalho A M G, Gandra F C G, von Ranke P J and de Oliveira N A 2004 *Phys. Rev. Lett.* **93** 237202

[66] Webster P J, Ziebeck K R A, Town S L and Peak M S 1984 *Phil. Mag.* B **49** 295

[67] Hu F X, Shen B G, Sun J R and Wu G H 2001 *Phys. Rev.* B **64** 132412

[68] Marcos J, Planes A, Manosa L, Casanova F, Batlle X, Labarta A and Martinez B 2002 *Phys. Rev.* B **66** 224413

[69] Kuo Y K, Sivakumar K M, Chen H C, Su J H and Lue C S 2005 *Phys. Rev.* B **72** 054116

[70] Zhou X Z, Li W, Kunkel H P, Williams G and Zhang S H 2005 *J. Appl. Phys.* **97** 10M515

[71] Long Y, Zhang Z Y, Wen D, Wu G H, Ye R C, Chang Y Q and Wan F R 2005 *J. Appl. Phys.* **98** 033515

[72] Fujii H, Komura S, Katega T, Okamoto T, I Y and Akimitsu J 1979 *J. Phys. Soc. Japan* **46** 1616

[73] Fujii H, Hokabe T, Komigaichi T and Okamoto T 1977 *J. Phys. Soc. Japan* **43** 41

[74] Kadomatsu H, Isoda M, Tohma K, Fujii H, Okamoto T and Fujiwara H 1985 *J. Phys. Soc. Japan* **54** 2790

[75] Jernberg P, Yousif A and Hägström L 1984 *J. Solid State Chem.* **53** 313

[76] Beckmann O and Lundgren L 1991 *Handbook of Magnetic Materials* vol 6, ed K H J Buschow (Amsterdam: North Holland) pp 181–287

[77] Brück E, Tegus O, Li X W, de Boer F R and Buschow K H J 2003 *Physica B: Condens. Matter* **327** 431–7

[78] Tegus O, Brück E, Zhang L, Dagula, Buschow K H J and de Boer F R 2002 *Physica* B **319** 174–92

[79] Tegus O, Brück E, Dagula W, Li X W, Zhang L, Buschow K H J and de Boer F R 2003 *J. Appl. Phys.* **93** 7655–7

[80] Tegus O, Fuquan B, Dagula W, Zhang L, Brück E, Si P Z, de Boer F R and Buschow K H J 2005 *J. Alloys Compounds* **396** 6–9

[81] Zhang L, Moze O, Prokes K, Tegus O and Brück E 2005 *J. Magn. Magn. Mater.* **290** 679–81

[82] Bacmann M, Soubeyroux J L, Barrett R, Fruchart D, Zach R, Niziol S and Fruchart R 1994 *J. Magn. Magn. Mater.* **134** 59–67

[83] Tegus O, Brück E, Buschow K H J and de Boer F R 2002 *Nature* **415** 150–2
[84] Pecharsky V K, Gschneider K A, Pecharsky A O and Tishin A M 2001 *Phys. Rev.* B **64** 144406
[85] Dagula W, Tegus O, Li X W, Song L, Brück E, Cam Thanh D T, de Boer F R and Buschow K H J 2006 *J. Appl. Phys.* at press
[86] Cam Thanh D T, Brück E, Tegus O, Klaasse J C P, Gortenmulder T J and Buschow K H J 2006 *J. Appl. Phys.* at press
[87] Samolyuk G D and Antropov V P 2005 *J. Appl. Phys.* **97** 10A310
[88] Pecharsky V K and Gschneidner K A 2001 *J. Appl. Phys.* **90** 4614–22
[89] Brück E, Ilyn M, Tishin A M and Tegus O 2005 *J. Magn. Magn. Mater.* **290** 8–13
[90] Tegus O, Brück E, Li X W, Zhang L, Dagula W, de Boer F R and Buschow K H J 2004 *J. Magn. Magn. Mater.* **272–276** 2389–90
[91] Gschneidner K A, Pecharsky V K and Tsokol A O 2005 *Rep. Prog. Phys.* **68** 1479–539
[92] Tohei T, Wada H and Kanomata T 2003 *J. Appl. Phys.* **94** 1800–2
[93] Dan'kov S Y, Tishin A M, Pecharsky V K and Gschneidner K A 1998 *Phys. Rev.* B **57** 3478–90
[94] Hu F X, Shen B G, Sun J R, Wang G J and Cheng Z H 2002 *Appl. Phys. Lett.* **80** 826–9
[95] Casanova F and Fernandez I 2004 *PhD Thesis* University of Barcelona
[96] Dagula W, Tegus O, Fuquan B, Zhang L, Si P Z, Zhang M, Zhang W S, Brück E, de Boer F R and Buschow K H J 2005 *IEEE Trans. Magn.* **41** 2778–80